

# Waveform relaxation for functional-differential equations

*Barbara Zubik-Kowal*  
*Stefan Vandewalle*

*Report TW 275, January 1998*



**Katholieke Universiteit Leuven**  
Department of Computer Science  
Celestijnenlaan 200A – B-3001 Heverlee (Belgium)

# Waveform relaxation for functional-differential equations

*Barbara Zubik-Kowal*  
*Stefan Vandewalle*

*Report TW 275, January 1998*

Department of Computer Science, K.U.Leuven

## **Abstract**

The convergence of waveform relaxation techniques for solving functional-differential equations is studied. New error estimates are derived that hold under linear and nonlinear conditions for the right-hand side of the equation. Sharp error bounds are obtained under generalized time-dependent Lipschitz conditions. The convergence of the waveform method and the quality of the a priori error bounds are illustrated by means of extensive numerical data obtained by applying the method of lines to three partial functional-differential equations.

**Keywords :** waveform relaxation, functional differential equations, numerical method of lines, error estimates

**AMS(MOS) Classification :** 65L20, 65M20, 39B12

# WAVEFORM RELAXATION FOR FUNCTIONAL-DIFFERENTIAL EQUATIONS

BARBARA ZUBIK-KOWAL<sup>†</sup> AND STEFAN VANDEWALLE<sup>† ‡</sup>

**Abstract.** The convergence of waveform relaxation techniques for solving functional-differential equations is studied. New error estimates are derived that hold under linear and nonlinear conditions for the right-hand side of the equation. Sharp error bounds are obtained under generalized time-dependent Lipschitz conditions. The convergence of the waveform method and the quality of the a priori error bounds are illustrated by means of extensive numerical data obtained by applying the method of lines to three partial functional-differential equations.

**Key words.** waveform relaxation, functional differential equations, numerical method of lines, error estimates

**AMS subject classifications.** 65L20, 65M20, 39B12

**1. Introduction.** Waveform relaxation is an iterative method for systems of ordinary differential equations. It differs from classical iterative methods in that it iterates with functions in a function space, instead of with finite sets of discrete unknowns. The method dates back to the end of the last century, where it was used by Picard and Lindelöf to prove the existence of solutions to ordinary differential equations, see [12], [10]. As a practical numerical method it was first proposed by Lelarsmee et al. [9] in the context of electrical system simulation. Since then, the method has been considered for various applications by many authors. For a recent state-of-the-art we refer to the book by Burrage [3] and the overview paper by Miekka and Nevanlinna [11].

In this paper we study the application of the waveform relaxation (WR) technique for functional equations. Such problems arise for example in population dynamics, in the modelling of visco-elastic materials and in the study of nonlinear materials with memory. These equations include differential integral equations, delay differential equations as well as ordinary differential equations as special cases.

The numerical properties of the method as an iterative solver for delay equations were studied, e.g., by Feldstein, Iserles and Levin in [4], and by Bjørhus in [1]. The latter paper also includes error estimates of the continuous-time waveform method for nonlinear delay equations. The discrete-time waveform technique for ordinary differential equations is studied by Bjørhus in [2], for the forward and backward Euler methods with strict (i.e., constant) Lipschitz conditions imposed on the ODE right-hand side. The error estimates presented in our paper apply to the more general class of differential functional equations. The estimates are sharper than those of the above references, for two reasons. First, we consider generalized (i.e., time-dependent) Lipschitz conditions instead of strict Lipschitz conditions. Such type of condition was also employed by Sand and Burrage in [14], but in that reference differential equations without functional argument were considered. Next, even in the case of strict Lipschitz conditions we obtain sharper results because of a different use of the one-sided Lipschitz condition (in the case of a negative constant). A similar technique

---

<sup>†</sup>Katholieke Universiteit Leuven, Department of Computer Science, Celestijnenlaan 200A, B-3001 Heverlee, Belgium (barbara.zubik-kowal, stefan.vandewalle@cs.kuleuven.ac.be). This research has been funded by the Research Fund K.U.Leuven (OT/94/16) and the Fund for Scientific Research - Flanders, Belgium (F.W.O., project G.0235.96).

<sup>‡</sup>Postdoctoral Research Fellow of the Fund for Scientific Research - Flanders, Belgium (F.W.O.).

was used by Zennaro in [15], for equations without functional argument. The error bounds in our paper are given in an arbitrary norm.

The convergence of the waveform relaxation technique for functional equations of neutral type is studied by Jackiewicz, Kwapisz and Lo in [7]. Their general results can be applied to the type of equations considered in the present paper, yet that would lead to weaker estimates. We also mention the paper by Jackiewicz and Kwapisz [6], where the convergence of WR is studied when applied to differential-algebraic equations. Their proving technique is different from ours, however, as it is based on contraction mapping principle. Also, that paper does not deal with error bounds. In our work we also include results of actual computations, and validate the quality of the theoretical estimates by extensive numerical data. This is done by several examples from partial functional-differential equations of parabolic type.

The structure of the paper is as follows. The type of equation that we consider is defined in §2, and the application of the WR method for such problems is illustrated by means of three examples. Convergence of the iterative scheme under very general and nonlinear conditions is studied in §3, where also a very general error estimate is derived. The method's convergence under a generalized, time-dependent Lipschitz condition is analysed in §4. Error bounds for various special cases are derived, and compared to error estimates that are obtained under strict Lipschitz conditions. The quality of the different error estimates is illustrated graphically and compared to actual errors obtained in numerical experiments. We end with some concluding remarks in §5.

## 2. The waveform relaxation method.

**2.1. General iteration scheme.** We consider the following Cauchy problem for a system of ordinary differential-functional equations

$$(2.1) \quad \begin{aligned} \dot{y}(t) &= F(t, y(t), y_t), \quad t \in [0, T], \\ y(t) &= y_0(t), \quad t \in [-\tau_0, 0]. \end{aligned}$$

Here,  $F : [0, T] \times \mathbb{R}^n \times C([-\tau_0, 0], \mathbb{R}^n) \rightarrow \mathbb{R}^n$ , with  $T > 0$  and  $\tau_0 \geq 0$ , is a continuous function. The function  $y_t : [-\tau_0, 0] \rightarrow \mathbb{R}^n$  for  $t \in [0, T]$  and  $y \in C([-\tau_0, T], \mathbb{R}^n)$  is defined as

$$(2.2) \quad y_t(s) = y(t + s), \quad s \in [-\tau_0, 0].$$

Equation (2.1) is a very general type of equation and includes for example ordinary differential equations,

$$\dot{y}(t) = F(t, y(t)),$$

delay equations,

$$\dot{y}(t) = F(t, y(t), y(\theta(t))), \quad \text{with } -\tau_0 + t \leq \theta(t) \leq t,$$

and also integro-differential equations,

$$\dot{y}(t) = F(t, y(t), \int_{-\tau_0}^0 y(t+s) ds).$$

The general WR method for (2.1) is an iteration scheme of the following form

$$(2.3) \quad \begin{aligned} \dot{y}^{k+1}(t) &= H(t, y^{k+1}(t), y^k(t), y_t^{k+1}, y_t^k), \quad t \in [0, T], \\ y^{k+1}(t) &= y_0(t), \quad t \in [-\tau_0, 0], \end{aligned}$$

where  $k = 0, 1, 2, \dots$  and where  $y^0$  is a given starting function. The function  $H$ , which is called the splitting function, is chosen to attempt to decouple system (2.1) into easily solvable independent subsystems, which may then be solved separately. In the present paper, we will study a somewhat more restricted class of methods, namely

$$(2.4) \quad \begin{aligned} \dot{y}^{k+1}(t) &= G(t, y^{k+1}(t), y^k(t), y_t^k), \quad t \in [0, T], \\ y^{k+1}(t) &= y_0(t), \quad t \in [-\tau_0, 0]. \end{aligned}$$

That is, the functional argument is always taken from a previous iterate. In this way we completely avoid having to solve any functional equations at all during the iteration. The splitting function  $G$  is minimally assumed to satisfy a consistency condition, which ensures that the solution to (2.1) is a fixed point of (2.4).

ASSUMPTION 1. *The function  $G : [0, T] \times \mathbb{R}^n \times \mathbb{R}^n \times C([-\tau_0, 0], \mathbb{R}^n) \rightarrow \mathbb{R}^n$  satisfies*

$$(2.5) \quad G(t, p(t), p(t), p_t) = F(t, p(t), p_t),$$

for any function  $p \in C([-\tau_0, T], \mathbb{R}^n)$ .

For example, the Jacobi/Picard WR scheme

$$(2.6) \quad \dot{y}_i^{k+1}(t) = F_i(t, y_1^k(t), \dots, y_{i-1}^k(t), y_i^{k+1}(t), y_{i+1}^k(t), \dots, y_n^k(t), y_t^k), \quad i = 1, \dots, n,$$

and the Gauss-Seidel/Picard WR scheme

$$(2.7) \quad \dot{y}_i^{k+1}(t) = F_i(t, y_1^{k+1}(t), \dots, y_i^{k+1}(t), y_{i+1}^k(t), \dots, y_n^k(t), y_t^k), \quad i = 1, \dots, n,$$

can be obtained for particular choices of the splitting function  $G$  in (2.4). Scheme (2.6) is parallel; (2.7) is sequential. As the functional term is taken from the previous iteration, we have added the term ‘Picard’ to the names of the schemes.

**2.2. Three numerical experiments.** In order to illustrate the WR procedure we will consider three examples. They are problems of type (2.1), that are derived by replacing the spatial derivatives in a *partial* differential-functional problem by finite difference methods. The convergence of this *numerical method of lines* for differential-functional problems, i.e., convergence of the solution of the functional-ODE to the solution of the functional PDE, is studied for instance in [16] and [17].

**2.2.1. Example 1: An integro-differential equation with an integral in time.** We apply the numerical method of lines to the following initial-boundary value problem for  $(t, x) \in [0, 10] \times [-L, L]$ ,

$$(2.8) \quad \frac{\partial}{\partial t} u(t, x) = \frac{1}{8(1+2t)} \frac{\partial^2}{\partial x^2} u(t, x) + \frac{1}{1+2t} \int_{-1}^0 u(t+s, x) ds + g(t, x),$$

with the following initial and boundary conditions,

$$u(t, x) = t x^2, \quad (t, x) \in [-1, 0] \times [-L, L] \quad \text{and} \quad u(t, \pm L) = t L^2, \quad t \in (0, 10].$$

The right-hand side function  $g(t, x)$  is chosen in such a way that the solution of the equation is known exactly and equal to  $u(t, x) = t x^2$ . After spatial discretization a system of ordinary differential-functional equations results,

$$(2.9) \quad \dot{v}_i(t) = \frac{v_{i+1}(t) - 2v_i(t) + v_{i-1}(t)}{8h^2(1+2t)} + \frac{1}{1+2t} \int_{-1}^0 v_i(t+s) ds + g_i(t),$$

for  $i = -M + 1, \dots, M - 1$ , with given initial and boundary values

$$v_i(t) = t i^2 h^2, \quad t \in [-1, 0] \quad \text{and} \quad v_{-M}(t) = v_M(t) = t L^2, \quad t \in (0, 10].$$

Here,  $h$  is the spatial step;  $M$  is a natural number such that  $Mh = L$ ;  $g_i(t) = g(t, ih)$ , and  $v_i(t)$  is meant to approximate the solution of (2.8) at the point  $(t, ih)$ .

We consider three different iteration schemes: Jacobi/Picard,

$$\dot{v}_i^{k+1}(t) = \frac{v_{i+1}^k(t) - 2v_i^{k+1}(t) + v_{i-1}^k(t)}{8h^2(1+2t)} + \frac{1}{1+2t} \int_{-1}^0 v_i^k(t+s) ds + g_i(t),$$

Gauss-Seidel/Picard,

$$\dot{v}_i^{k+1}(t) = \frac{v_{i+1}^k(t) - 2v_i^{k+1}(t) + v_{i-1}^{k+1}(t)}{8h^2(1+2t)} + \frac{1}{1+2t} \int_{-1}^0 v_i^k(t+s) ds + g_i(t),$$

and a third scheme that treats the functional part of the equation in a Picard way, but does not split the ODE part,

$$\dot{v}_i^{k+1}(t) = \frac{v_{i+1}^{k+1}(t) - 2v_i^{k+1}(t) + v_{i-1}^{k+1}(t)}{8h^2(1+2t)} + \frac{1}{1+2t} \int_{-1}^0 v_i^k(t+s) ds + g_i(t).$$

We refer to the latter as the ‘direct/Picard’ scheme. For each iteration we have in addition that the iterates satisfy the initial and boundary conditions

$$v_i^{k+1}(t) = t i^2 h^2, \quad t \in [-1, 0] \quad \text{and} \quad v_{-M}^{k+1}(t) = v_M^{k+1}(t) = t L^2, \quad t \in (0, 10].$$

The starting function is selected as  $v_i^0(t) = t L^2$ ,  $t \in [0, 10]$ .

The exact solution of problem (2.8) is a low order polynomial; the spatial discretization is such that no discretization error is made. Hence, the exact solution to (2.9) is given by  $v_i(t) = t i^2 h^2$ . Let  $\tilde{v}^k(t, ih)$ , denote the  $k$ -th numerical approximate solution of either of the three waveform methods obtained with application of numerical integration for the time integral and a numerical method for solving the systems of ODEs. We define the numerical error as

$$(2.10) \quad \tilde{e}^k(t) = \max_{i=-M, \dots, M} \{|\tilde{v}^k(t, ih) - u(t, ih)|\}, \quad t \in [0, T].$$

This error has a discretization error component and a WR iteration error component. Upon convergence of the iteration scheme the latter will obviously vanish; in this particular example also the discretization error becomes zero.

The evolution of the *error at time-point*  $t = 10$  for the three different waveform schemes is illustrated in Figure 2.1. For the computation in the picture to the left, we selected  $L = 1$ ,  $M = 10$ , and hence  $h = 0.1$ . We used the composite trapezoidal rule for computing the integral and the explicit Adams method of order four with time step  $\Delta t = 0.01$  for numerical integration of the ODEs. In the second picture of Figure 2.1 we show analogous results obtained with different discretization parameters. In that case,  $L = 10$ ,  $M = 100$  and  $h = 0.1$ . Numerical integration was again with the composite trapezoidal rule but the ODE solution was done with the third order (implicit) backward differentiation scheme (BDF3) with time-step  $\Delta t = 0.1$ . The evolution of the *error as function of time* for  $t \in [0, 10]$  for different values of the iteration index  $k$  is shown in Figure 2.2. For these computations we used the composite trapezoidal rule and BDF3 with  $\Delta t = 0.1$ . The numerical experiments from Figure 2.1 and Figure 2.2 are made for the infinity norm. The theoretical results from the next sections will apply for arbitrary norms.

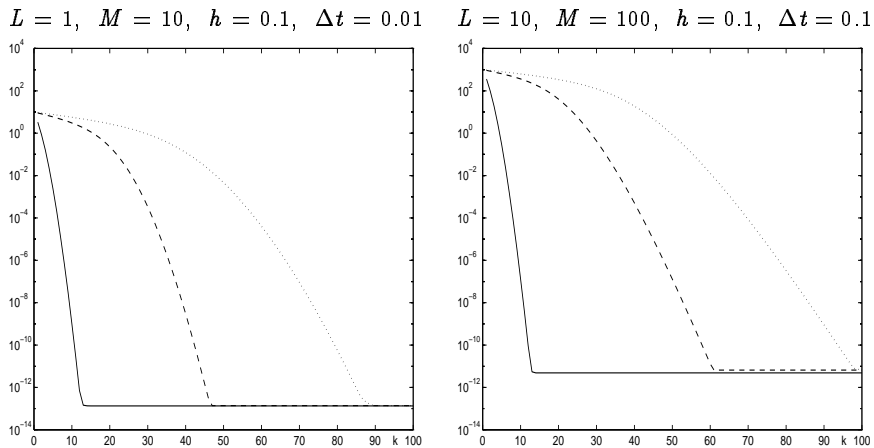


FIG. 2.1. Numerical error (2.10) at  $t=10$  as a function of the iteration index  $k$ , for Example 1 and for three different WR methods: Jacobi/Picard (dotted), Gauss-Seidel/Picard (dashed), and direct/Picard (solid). The two pictures correspond to different discretization parameters (e.g., system of 21 ODEs (left), and system of 201 ODEs (right)).

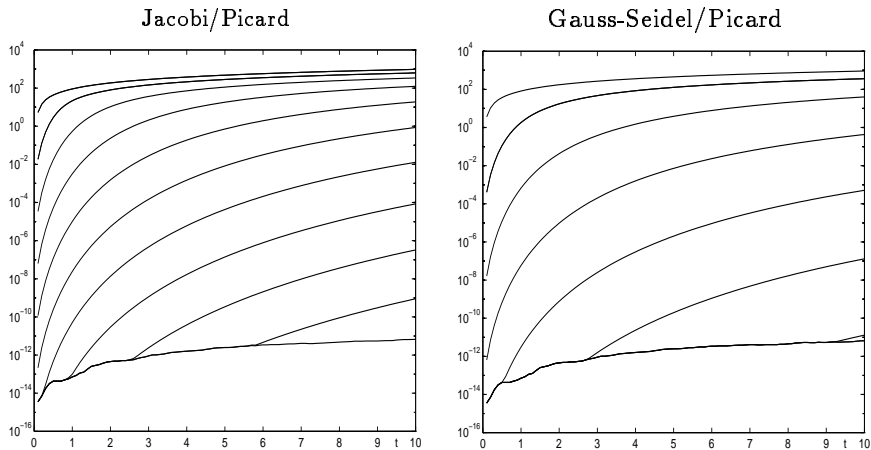


FIG. 2.2. Numerical error (2.10) as a function of  $t \in [0, 10]$  for Example 1, with  $L = 10$ ,  $M = 100$ ,  $h = 0.1$ ,  $\Delta t = 0.1$ . The error  $\tilde{e}^k(t)$  is plotted for different values of the iteration index  $k = 1, 10, 20, \dots, 100$ .

**2.2.2. Example 2: An integro-differential equation with an integral in space and a constant delay in time.** The next problem is defined for  $t \in [0, 10]$  and  $x \in [-10, 10]$ ,

$$(2.11) \quad \frac{\partial}{\partial t} u(t, x) = \frac{e^{-2t}}{8} \frac{\partial^2}{\partial x^2} u(t, x) + e^{-2t} \int_{-1}^1 u(t-1, x+s) ds + g(t, x),$$

with given initial and boundary values on the region

$$(2.12) \quad (t, x) \in ([-1, 0] \times [-11, 11]) \cup ([0, 10] \times ([-11, -10] \cup [10, 11])) .$$

The function  $g(t, \mathbf{x})$  and the initial and boundary values are selected in such a way that the exact solution becomes

$$u(t, \mathbf{x}) = \sin(\pi t) \sin(\pi \mathbf{x}) .$$

We apply the numerical method of lines and the composite trapezoidal formula for the integral with respect to spatial variable. This leads to a discrete set of delay differential equations of the form

$$\dot{v}_i(t) = \frac{e^{-2t}}{8h^2} [v_{i+1}(t) - 2v_i(t) + v_{i-1}(t)] + \frac{h}{2} e^{-2t} \sum_{j=-N}^{N-1} [v_{i+j}(t-1) + v_{i+j+1}(t-1)] + g(t, \mathbf{x}) .$$

Application of the Jacobi/Picard scheme (2.6), leads to the iteration formula

$$(2.13) \quad \begin{aligned} \dot{v}_i^{k+1}(t) &= \frac{e^{-2t}}{8h^2} [v_{i+1}^k(t) - 2v_i^{k+1}(t) + v_{i-1}^k(t)] \\ &+ \frac{h}{2} e^{-2t} \sum_{j=-N}^{N-1} [v_{i+j}^k(t-1) + v_{i+j+1}^k(t-1)] + g_i(t) , \end{aligned}$$

for  $t \in [0, 10]$ . The initial-boundary condition of Dirichlet type is

$$v_i^{k+1}(t) = \sin(\pi t) \sin(\pi i h) , \quad i = -M - N, \dots, M + N ,$$

for any values of  $t$  for which  $(t, i h)$  is in the initial-boundary region (2.12). Here,  $g_i(t) = g(t, i h)$  and  $M, N$  are natural numbers such that  $M h = 10$ ,  $N h = 1$ . As the initial iterate we select  $v^0 \equiv 0$  on  $[0, 10] \times [-10, 10]$ . Note that, for fixed  $k$ , system (2.13) is a trivially solvable system of decoupled, scalar ordinary differential equations. In a similar way, one can immediately construct the Gauss-Seidel/Picard and direct/Picard waveform methods.

In the first picture of Figure 2.3 we show the evolution of the numerical error (2.10) at  $t = 10$  as a function of the iteration index  $k$ . The results were obtained with  $h = 0.1$ ,  $M = 100$ ,  $N = 10$  and application of BDF3 with time step  $\Delta t = 0.1$ . Note that the method of lines applied to (2.11) is of second order accuracy. Hence, for large  $k$  the discretization error remains, while the WR iteration error, defined as

$$(2.14) \quad \hat{e}^k(t) = \max_{i=-M, \dots, M} \{|v^k(t, i h) - v(t, i h)|\} .$$

vanishes. To illustrate this effect, we have in the second picture of Figure 2.3 separated both error components and only plotted the iteration component of the error.

The evolution of the errors (either (2.10) or (2.14)) as functions of  $t \in [0, 10]$  for different  $k$  is shown in Figure 2.4. The computation was performed with  $h = 0.1$  and BDF3 with  $\Delta t = 0.1$ .

**2.2.3. Example 3: A delay differential equation with constant delay in time.** Next, we consider a partial differential equation with a constant delay argument

$$(2.15) \quad \frac{\partial}{\partial t} u(t, \mathbf{x}) = \frac{1}{10 + 40t^2} \frac{\partial^2}{\partial \mathbf{x}^2} u(t, \mathbf{x}) + e^{-4t^2} u(t-1, \mathbf{x}) + g(t, \mathbf{x}) ,$$

for  $t \in [0, 10]$ . Initial and boundary conditions are imposed on the region

$$(2.16) \quad (t, \mathbf{x}) \in ([-1, 0] \times [-10, 10]) \cup ([0, 10] \times \{-10, 10\}) .$$

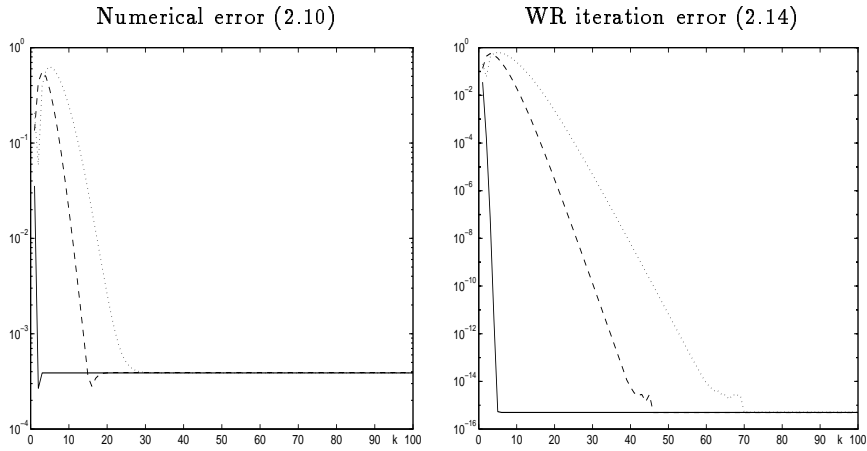


FIG. 2.3. Errors (2.10) and (2.14) for  $k = 1, 2, \dots, 100$ , at  $t = 10$  for Example 2 with Jacobi/Picard (dotted), Gauss-Seidel/Picard (dashed), and direct/Picard (solid) waveform relaxation ( $M = 100$ ,  $N = 10$ ,  $h = \Delta t = 0.1$ ).

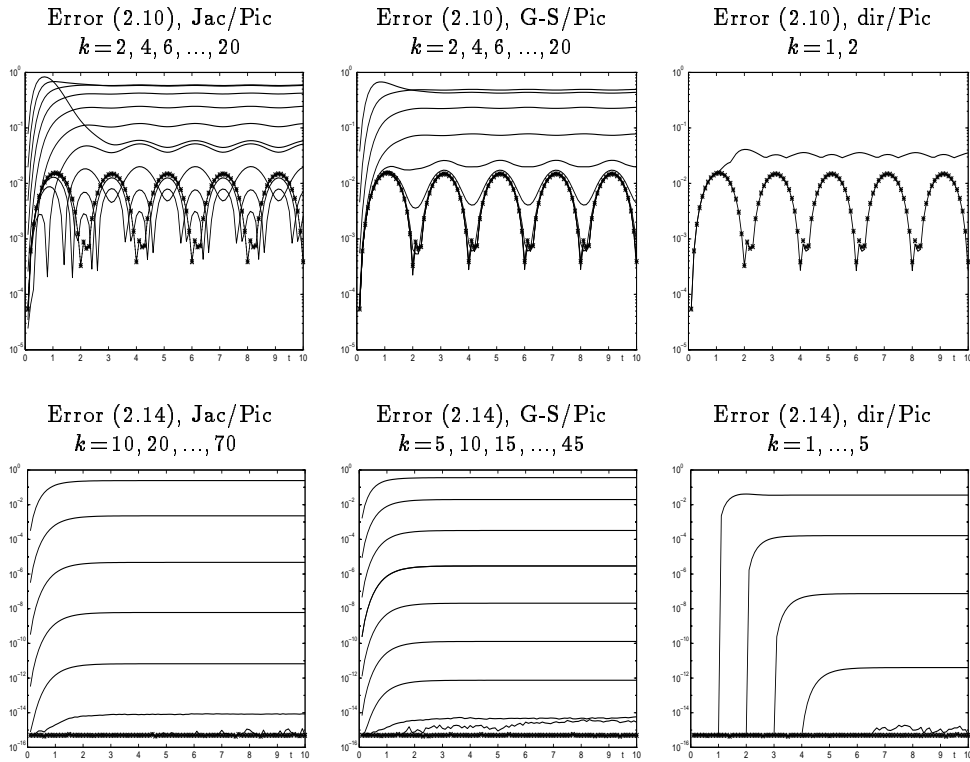


FIG. 2.4. Errors as a function of time for  $t \in [0, 10]$  for Example 2 ( $h = \Delta t = 0.1$ ). The \*'s indicate values obtained for  $k = 100$ .

The function  $g(t, \mathbf{x})$  and the initial and boundary values are selected in such a way that the exact solution becomes

$$u(t, \mathbf{x}) = te^{-\mathbf{x}^2}.$$

After application of the numerical method of lines we obtain for the Jacobi/Picard WR scheme the following iteration formula

$$\dot{v}_i^{k+1}(t) = \frac{h^{-2}}{10 + 40t^2} [v_{i+1}^k(t) - 2v_i^{k+1}(t) + v_{i-1}^k(t)] + e^{-4t^2} v_i^k(t-1) + g_i(t),$$

for  $t \in [0, 10]$ ,  $i = -M + 1, \dots, M - 1$ , with initial-boundary condition taken from the true solution. In a similar way the Gauss-Seidel/Picard and direct/Picard schemes can be defined.

We took  $h = 0.1$  for the numerical method of lines and used BDF3 with  $\Delta t = 0.1$  for the numerical integration of the ODEs. The evolution of the error obtained after the computation as a function of  $k$  for fixed  $t = 10$  is shown in Figure 2.5. In the second picture only the iteration error is plotted while in the first one the whole error (2.10) is shown. The numerical error (2.10) and WR iteration error (2.14) as functions of  $t \in [0, 10]$  are presented respectively in the first and second rows of Figure 2.6.

**3. A general assumption and error estimate.** In the current and in the next section we will derive theoretical estimates for the actual iteration errors defined as  $e^k(t) = \mathbf{y}^k(t) - \mathbf{y}(t)$ , where  $\mathbf{y}(t)$  is the solution to (2.1) and  $\mathbf{y}^k(t)$  is the  $k$ -th iterate obtained with scheme (2.4). The estimates will be given for an arbitrary norm in  $\mathbb{R}^n$ . The assumption below will be needed throughout the paper. In its formulation we use the notation  $\|\cdot\|_0$ , defined as

$$\|r\|_0 = \max_{s \in [-\tau_0, 0]} \|r(s)\|.$$

ASSUMPTION 2. *The function  $G : [0, T] \times \mathbb{R}^n \times \mathbb{R}^n \times C([-\tau_0, 0], \mathbb{R}^n) \rightarrow \mathbb{R}^n$  satisfies*

$$(3.1) \quad \|\mathbf{p} - \bar{\mathbf{p}} - \nu[G(t, \mathbf{p}, \mathbf{q}, \mathbf{r}) - G(t, \bar{\mathbf{p}}, \mathbf{q}, \mathbf{r})]\| \geq (1 - \nu\mu_1(t))\|\mathbf{p} - \bar{\mathbf{p}}\|,$$

$$(3.2) \quad \|G(t, \mathbf{p}, \mathbf{q}, \mathbf{r}) - G(t, \mathbf{p}, \bar{\mathbf{q}}, \mathbf{r})\| \leq \mu_2(t)\|\mathbf{q} - \bar{\mathbf{q}}\|,$$

$$(3.3) \quad \|G(t, \mathbf{p}, \mathbf{q}, \mathbf{r}) - G(t, \mathbf{p}, \mathbf{q}, \bar{\mathbf{r}})\| \leq \sigma(t, \|\mathbf{r} - \bar{\mathbf{r}}\|_0),$$

for  $\nu \geq 0$ ,  $t \in [0, T]$ ,  $\mathbf{p}, \bar{\mathbf{p}}, \mathbf{q}, \bar{\mathbf{q}} \in \mathbb{R}^n$ ,  $\mathbf{r}, \bar{\mathbf{r}} \in C([-\tau_0, 0], \mathbb{R}^n)$ ; the functions  $\mu_1 : [0, T] \rightarrow \mathbb{R}$  and  $\mu_2 : [0, T] \rightarrow \mathbb{R}_+$  are continuous; the function  $\sigma : [0, T] \times \mathbb{R}_+ \rightarrow \mathbb{R}_+$  is continuous and nondecreasing with respect to the second argument;  $\|\cdot\|$  is an arbitrary norm in  $\mathbb{R}^n$ .

The splitting functions  $G$  for the three waveform schemes considered in the three examples satisfy the above assumption for the functions  $\mu_1$ ,  $\mu_2$ , and  $\sigma$  as given in Table 3.1, and this for the infinity and the Euclidean norm. The same schemes also satisfy conditions (3.1)-(3.3) with constant values for  $\mu_1$  and  $\mu_2$ , and with the time-independent function  $\sigma$  as given in Table 3.2. We will show that if one chooses the functions from Table 3.1 one arrives at substantially sharper error bounds than when one selects the values from Table 3.2. We also want to point out that, thanks to one-sided nature of the Lipschitz condition, the function  $\mu_1$  is negative for the Jacobi and the Gauss-Seidel schemes. We will show further on that negative values for  $\mu_1$  make the error bounds a factor  $\exp\left(\int_0^t \mu_1(s) ds\right)$  smaller than the ones given in [1].

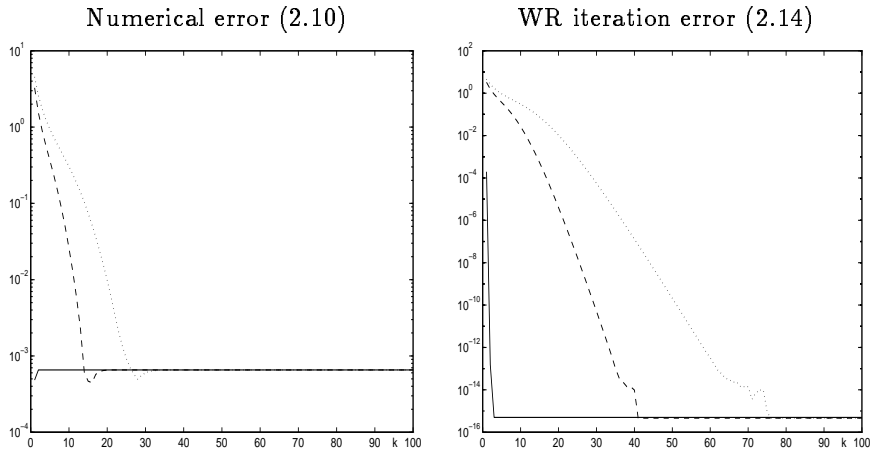


FIG. 2.5. Errors (2.10) and (2.14) for  $k = 1, 2, \dots, 100$ , at  $t = 10$  for Example 3 with Jacobi/Picard (dotted), Gauss-Seidel/Picard (dashed), and direct/Picard (solid) waveform relaxation ( $M = 100$ ,  $h = \Delta t = 0.1$ ).

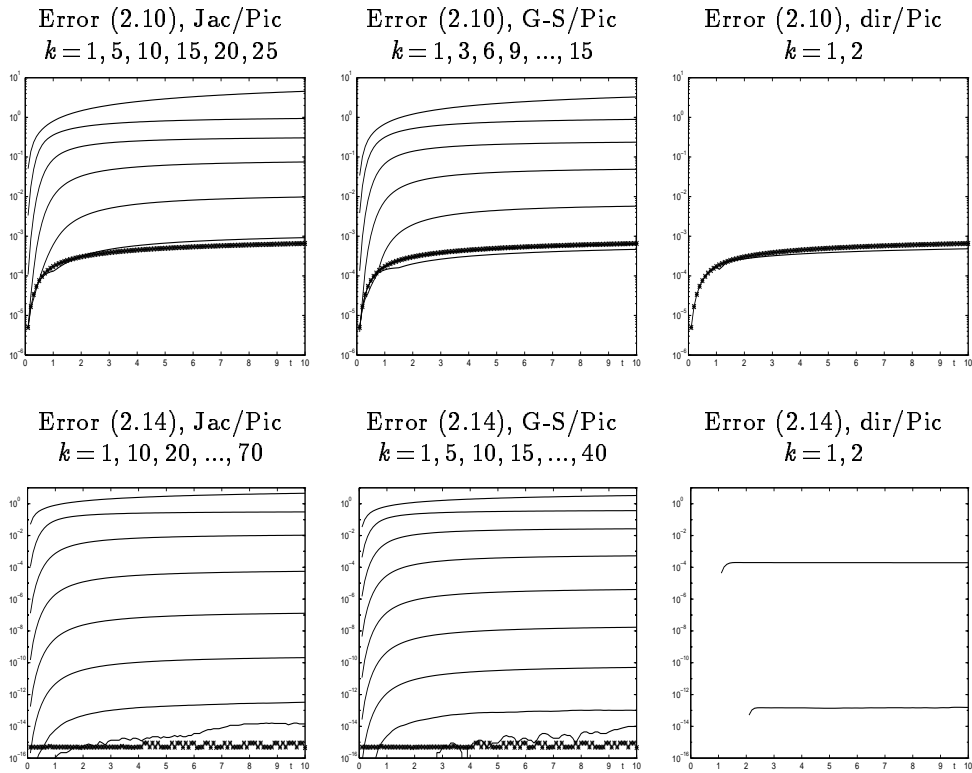


FIG. 2.6. Errors as a function of time for  $t \in [0, 10]$  for Example 3 ( $h = \Delta t = 0.1$ ). The \*'s indicate values for  $k = 100$ .

TABLE 3.1

Time-dependent functions  $\mu_1$ ,  $\mu_2$  and  $\sigma$ , satisfying conditions (3.1)-(3.3) for Jacobi/Picard, Gauss-Seidel/Picard and direct/Picard schemes for Examples 1, 2, and 3.

Coeff.	Example 1			Example 2			Example 3		
	Jac	G-S	dir	Jac	G-S	dir	Jac	G-S	dir
$\mu_1(t)$	$\frac{-h^{-2}}{4(1+2t)}$	$\frac{-h^{-2}}{8(1+2t)}$	0	$\frac{-h^{-2}}{4e^{2t}}$	$\frac{-h^{-2}}{8e^{2t}}$	0	$\frac{-h^{-2}}{5(1+4t^2)}$	$\frac{-h^{-2}}{10(1+4t^2)}$	0
$\mu_2(t)$	$\frac{h^{-2}}{4(1+2t)}$	$\frac{h^{-2}}{8(1+2t)}$	0	$\frac{h^{-2}}{4e^{2t}}$	$\frac{h^{-2}}{8e^{2t}}$	0	$\frac{h^{-2}}{5(1+4t^2)}$	$\frac{h^{-2}}{10(1+4t^2)}$	0
$\sigma(t, w)$	$\frac{w}{1+2t}$	$\frac{w}{1+2t}$	$\frac{w}{1+2t}$	$\frac{2w}{e^{2t}}$	$\frac{2w}{e^{2t}}$	$\frac{2w}{e^{2t}}$	$\frac{w}{e^{4t^2}}$	$\frac{w}{e^{4t^2}}$	$\frac{w}{e^{4t^2}}$

TABLE 3.2

Time-independent functions  $\mu_1$ ,  $\mu_2$  and  $\sigma$ , that satisfy conditions (3.1)-(3.3) for Jacobi/Picard, Gauss-Seidel/Picard and direct/Picard schemes for Examples 1, 2, and 3.

Coeff.	Example 1			Example 2			Example 3		
	Jac	G-S	dir	Jac	G-S	dir	Jac	G-S	dir
$\mu_1$	$\frac{-h^{-2}}{4}$	$\frac{-h^{-2}}{8}$	0	$\frac{-h^{-2}}{4}$	$\frac{-h^{-2}}{8}$	0	$\frac{-h^{-2}}{5}$	$\frac{-h^{-2}}{10}$	0
$\mu_2(t)$	$\frac{h^{-2}}{4}$	$\frac{h^{-2}}{8}$	0	$\frac{h^{-2}}{4}$	$\frac{h^{-2}}{8}$	0	$\frac{h^{-2}}{5}$	$\frac{h^{-2}}{10}$	0
$\sigma(t, w)$	$w$	$w$	$w$	$2w$	$2w$	$2w$	$w$	$w$	$w$

REMARK 3.1. Consider a functional parabolic problem of type

$$(3.4) \quad \frac{\partial}{\partial t} u(t, x) = a(t) \frac{\partial^2}{\partial x^2} u(t, x) + f(t, x, u(t, x)).$$

By specializing the function  $f$  one can obtain equations (2.8), (2.11), (2.15). The function  $u(t, x)$ , for  $(t, x) \in [0, T] \times [-L, L]$ , is defined by

$$(3.5) \quad u_{(t, x)}(\tau, s) = u(t + \tau, x + s), \quad (\tau, s) \in [-\tau_0, 0] \times [-\bar{\tau}_0, \bar{\tau}_0].$$

After application of the method of lines and a linear interpolating operator  $T_h$  (the properties of the operator in the multidimensional case are given in [17]) we obtain

$$(3.6) \quad \dot{u}_i(t) = \frac{a(t)}{h^2} [u_{i+1}(t) - u_i(t) + u_{i-1}(t)] + f(t, ih, T_h u_{(t, i)}),$$

where the function  $u_{(t, i)}$ , for  $t \in [0, T]$  and integer  $i$  such that  $ih \in [-L, L]$ , is defined by

$$(3.7) \quad u_{(t, i)}(\tau, jh) = u(t + \tau, (i + j)h), \quad (\tau, jh) \in [-\tau_0, 0] \times [-\bar{\tau}_0, \bar{\tau}_0].$$

In equation (3.4) we suppose that  $a \in C([0, T], \mathbb{R}_+)$  and  $f \in C([0, T] \times [-L, L] \times C([-\tau_0, 0] \times [-\bar{\tau}_0, \bar{\tau}_0], \mathbb{R}), \mathbb{R})$ ,  $\tau_0, \bar{\tau}_0 \geq 0$ ,  $L > 0$ . If we consider the Gauss-Seidel/Picard scheme for (3.6), then we have problem (2.1) with right-hand side  $G$  defined componentwise by

$$G_i(t, p, q, r) = \frac{a(t)}{h^2} [q_{i+1} - 2p_i + p_{i-1}] + f(t, ih, T_h(V_i r)),$$

where  $V_i(r)(\tau, jh) = r_{i+j}(\tau)$  for such integers  $i, j$  that  $ih \in [-L, L]$  and  $jh \in [-\bar{\tau}_0, \bar{\tau}_0]$  and for  $\tau \in [-\tau_0, 0]$ . We choose the infinity norm for  $\|\cdot\|$ . One can then derive that

$\mu_1(t) = \frac{-a(t)}{h^2}$ ,  $\mu_2(t) = \frac{a(t)}{h^2}$ . If we also assume that the function  $f$  in the right-hand side of (3.4) satisfies the condition

$$(3.8) \quad |f(t, x, w) - f(t, x, \bar{w})| \leq \sigma(t, \max_{[-\tau_0, 0] \times [-\bar{\tau}_0, \bar{\tau}_0]} |w(\tau, s) - \bar{w}(\tau, s)|),$$

for any  $w, \bar{w} \in C([- \tau_0, 0] \times [-\bar{\tau}_0, \bar{\tau}_0], \mathbb{R})$  then condition (3.3) is satisfied.

Assumption 2, together with the consistency condition formulated in Assumption 1, implies the following two Lemmas.

LEMMA 3.1. *Under Assumptions 1 and 2, the WR iteration error satisfies, for  $t \in [0, T]$ ,*

$$(3.9) \quad D^- \|e^{k+1}(t)\| \leq \mu_1(t) \|e^{k+1}(t)\| + \mu_2(t) \|e^k(t)\| + \sigma(t, \|e_t^k\|_0),$$

where  $D^-$  means the left derivative w.r.t.  $t$ , and where  $\|\cdot\|$  is an arbitrary norm.

*Proof.* We begin by the observation that

$$\begin{aligned} D^- \|e^{k+1}(t)\| &= \lim_{\nu \rightarrow 0^-} \frac{1}{\nu} \{ \|e^{k+1}(t+\nu)\| - \|e^{k+1}(t)\| \} \\ &= \lim_{\nu \rightarrow 0^-} \frac{1}{\nu} \{ \|e^{k+1}(t) + \nu \dot{e}^{k+1}(t)\| - \|e^{k+1}(t)\| \} \\ &= \lim_{\nu \rightarrow 0^-} \frac{1}{\nu} \{ \|e^{k+1}(t) + \nu [G(t, y^{k+1}(t), y(t), y_t) - G(t, y(t), y(t), y_t)] \\ &\quad + \nu [G(t, y^{k+1}(t), y^k(t), y_t) - G(t, y^{k+1}(t), y(t), y_t)] \\ &\quad + \nu [G(t, y^{k+1}(t), y^k(t), y_t^k) - G(t, y^{k+1}(t), y^k(t), y_t)] \| - \|e^{k+1}(t)\| \} \end{aligned}$$

which can be bounded from above by

$$\begin{aligned} &\lim_{\nu \rightarrow 0^-} \frac{1}{\nu} \{ \|e^{k+1}(t) + \nu [G(t, y^{k+1}(t), y(t), y_t) - G(t, y(t), y(t), y_t)] \\ &\quad + \nu \|G(t, y^{k+1}(t), y^k(t), y_t) - G(t, y^{k+1}(t), y(t), y_t)\| \\ &\quad + \nu \|G(t, y^{k+1}(t), y^k(t), y_t^k) - G(t, y^{k+1}(t), y^k(t), y_t)\| - \|e^{k+1}(t)\| \}. \end{aligned}$$

Now (3.9) is clear from (3.1)-(3.3).  $\square$

REMARK 3.2. If  $f \equiv 0$  in (3.4), then one can obtain  $\mu_1(t) = \frac{-a(t)}{h^2}$ ,  $\mu_2(t) = \frac{a(t)}{h^2}$  for the Gauss-Seidel/Picard scheme and  $\mu_1(t) = \frac{-2a(t)}{h^2}$ ,  $\mu_2(t) = \frac{2a(t)}{h^2}$  for the Jacobi/Picard scheme and  $\sigma \equiv 0$  for both of the schemes in (3.9) with an arbitrary norm  $\|\cdot\|$ .

Having (3.9) we can apply Gronwall's Lemma, and obtain the following result.

LEMMA 3.2. *Under Assumptions 1 and 2, the WR iteration error satisfies, for  $t \in [0, T]$ ,*

$$(3.10) \quad \|e^{k+1}(t)\| \leq \int_0^t \exp\left[\int_\tau^t \mu_1(s) ds\right] \{ \mu_2(\tau) \|e^k(\tau)\| + \sigma(\tau, \|e_\tau^k\|_0) \} d\tau.$$

With inequality (3.10) we can now proceed to prove convergence of the WR scheme (2.4), if also the additional assumption given below is satisfied. In the formulation of the assumption we use the notation  $|\cdot|_0$  which is defined as

$$(3.11) \quad |f|_0 = \max_{\tau \in [-\tau_0, 0]} |f(\tau)|.$$

ASSUMPTION 3. *The zero-function is the only solution of the problem*

$$(3.12) \quad \begin{cases} \omega'(t) = (\mu_1(t) + \mu_2(t)) \omega(t) + \sigma(t, |\omega_t|_0), & t \in [0, T], \\ \omega(t) = 0, & t \in [-\tau_0, 0]. \end{cases}$$

This assumption is satisfied for example in the case of  $\sigma(t, s) = \mu_3(t)s$ , where  $\mu_3 \in C([0, T], \mathbb{R}_+)$ , (see [5, Th.2.3]). The convergence theorem for functional differential equations is given next.

THEOREM 3.1. *Suppose that Assumptions 1, 2, and 3 are satisfied. Then,*

$$(3.13) \quad \|e^k(t)\| \leq w^k(t), \quad t \in [0, T], \quad k = 0, 1, 2, \dots,$$

where  $w^k(t) = 0$  for  $t \in [-\tau_0, 0]$ , and where  $w^k(t)$  is given recursively for  $t \in [0, T]$  and  $k = 0, 1, 2, \dots$  by

$$(3.14) \quad \begin{aligned} w^0(t) &= \max_{\tau \in [0, t]} \|e^0(\tau)\|, \\ w^{k+1}(t) &= \int_0^t \exp\left\{\int_\tau^t \mu_1(s) ds\right\} \{\mu_2(\tau) w^k(\tau) + \sigma(\tau, |w_\tau^k|_0)\} d\tau. \end{aligned}$$

Furthermore, if for some natural number  $k_0$

$$(3.15) \quad w^{k_0+1}(t) \leq w^{k_0}(t), \quad t \in [0, T],$$

then  $\lim_{k \rightarrow \infty} w^k(t) = 0$  uniformly with respect to  $t \in [0, T]$ .

*Proof.* Obviously, (3.13) is satisfied for  $k = 0$ . The result for  $k > 0$  follows from (3.10) by induction. Indeed, we have for  $t \in [0, T]$ ,

$$\|e^{k+1}(t)\| \leq \int_0^t \exp\left\{\int_\tau^t \mu_1(s) ds\right\} \{\mu_2(\tau) w^k(\tau) + \sigma(\tau, |w_\tau^k|_0)\} d\tau = w^{k+1}(t),$$

since by induction hypothesis we have  $\|e^k(\tau)\| \leq w^k(\tau)$  and  $\|e_\tau^k\|_0 \leq |w_\tau^k|_0$ .

In order to prove the second part of the theorem note that from (3.14), one has that the difference  $w^{k+1}(t) - w^k(t)$  equals

$$\int_0^t \exp\left\{\int_\tau^t \mu_1(s) ds\right\} (\mu_2(\tau) \{w^k(\tau) - w^{k-1}(\tau)\} + \sigma(\tau, |w_\tau^k|_0) - \sigma(\tau, |w_\tau^{k-1}|_0)) d\tau.$$

By using (3.15) and induction on  $k$ , it follows that this expression is negative for  $k \geq k_0$ , and hence

$$(3.16) \quad w^{k+1}(t) \leq w^k(t), \quad \text{for } k = k_0, k_0 + 1, \dots \text{ and } t \in [0, T].$$

Now we will show that  $\lim_{k \rightarrow \infty} w^k(t) = 0$ , uniformly w.r.t.  $t \in [0, T]$ . Since the function sequence  $\{w^k\}_{k=0}^\infty$  is uniformly bounded and equicontinuous on  $[0, T]$ , it contains (e.g., by Th. 7.25 in [13]) a uniformly convergent subsequence. From (3.14) and Assumption 3, one derives that this subsequence is uniformly convergent to zero. Hence, because of its boundedness and because of (3.16), the sequence  $\{w^k\}_{k=0}^\infty$  converges itself to zero pointwise. Thus, we have a sequence of continuous functions, that converge pointwise and monotonic to a continuous function on compact interval. By Th. 7.13 in [13] we may conclude that this sequence converges to the zero-function uniformly.  $\square$

REMARK 3.3. If  $\mu_1(t) + \mu_2(t) \geq 0$ , for  $t \in [0, T]$ , then the  $w^k$ -functions are non-decreasing, and thus  $|w_\tau^k|_0 = w^k(\tau)$ . Hence, definition (3.14) can be replaced by

$$w^{k+1}(t) = \int_0^t \exp\left[\int_\tau^t \mu_1(s) ds\right] (\mu_2(\tau)w^k(\tau) + \sigma(\tau, w^k(\tau))) d\tau,$$

a definition without functional arguments, and equation (3.12) can be replaced by

$$\omega'(t) = \sigma(t, \omega(t)) + (\mu_1(t) + \mu_2(t)) \omega(t).$$

REMARK 3.4. For the Jacobi/Picard and Gauss-Seidel/Picard schemes for (3.6) the equation in problem (3.12) simplifies to

$$\omega'(t) = \sigma(t, \omega(t)).$$

For examples of the function  $\sigma$  satisfying Assumption 3 we direct the reader to [8].

**4. A generalized, time-dependent Lipschitz condition.** Armed with the general theory outlined in the previous section, we will now derive error estimates for certain subclasses of problems. These estimates will be substantially sharper than the ones that are traditionally derived by using constant Lipschitz conditions.

**4.1. General error estimate.** In this section we consider the following condition as a special case of the general nonlinear condition given in (3.3),

$$(4.1) \quad \|G(t, p, q, r) - G(t, p, q, \bar{r})\| \leq \mu_3(t) \|r - \bar{r}\|_0,$$

with  $\mu_3 \in C([0, T], \mathbb{R}_+)$ . As we assume that  $\sigma(t, s)$  is of the form  $\mu_3(t)s$ , we know from the remark following the statement of Assumption 3 that the latter is satisfied. Additionally, we need the following assumptions on  $\mu_1, \mu_2$ , and  $\mu_3$ .

ASSUMPTION 4. *The function  $\mu_1$  is either strictly positive, strictly negative, or identically zero for  $t \in [0, T]$ . Either  $\mu_2$  or  $\mu_3$  (or both) does not have zeros in  $[0, T]$ .*

This assumption is satisfied by all of the iteration schemes considered in Examples 1, 2 and 3. With condition (4.1), we will be able to arrive at sharper bounds than under condition (3.3). The bound is presented in Theorem 4.1 and is given explicitly, whereas in Theorem 3.1 the error bound is given recursively. The proof is rather technical, and requires the use of different special functions for several different cases. The cases to be considered are

$$\left\{ \begin{array}{l} \text{case a: } \mu_1 \not\equiv 0 \\ \text{case b: } \mu_1 \equiv 0, \mu_2 \text{ has zeros, } \mu_3 \text{ has no zeros in } [0, T] \\ \text{case c: } \mu_1 \equiv 0, \mu_2 \text{ has no zeros, } \mu_3 \text{ has zeros in } [0, T] \\ \text{case d: } \mu_1 \equiv 0, \mu_2 \text{ has no zeros, } \mu_3 \text{ has no zeros in } [0, T] \end{array} \right.$$

The first set of functions needed in the analysis are the functions  $\Gamma_i : [0, T] \rightarrow \mathbb{R}_+$ ,

$$(4.2) \quad \Gamma_1(t) = \int_0^t \mu_1(\tau) d\tau, \quad \Gamma_2(t) = \int_0^t \mu_2(\tau) d\tau, \quad \Gamma_3(t) = \int_0^t \mu_3(\tau) d\tau.$$

We also need the functions  $\Lambda, \Omega, A_k : [0, T] \rightarrow \mathbb{R}_+$ , defined as follows:

case a:

$$\Lambda(t) = \max_{\tau \in [0, t]} \frac{\mu_2(\tau)}{|\mu_1(\tau)|}, \quad \Omega(t) = \max_{\tau \in [0, t]} \frac{\mu_3(\tau)}{|\mu_1(\tau)|}$$

$$A_k(t) = (-\text{sign}(\mu_1))^k \left[ 1 - e^{\Gamma_1(t)} \sum_{j=0}^{k-1} \frac{(-\Gamma_1(t))^j}{j!} \right]$$

case b:

$$\Lambda(t) = \max_{\tau \in [0, t]} \frac{\mu_2(\tau)}{\mu_3(\tau)}, \quad \Omega(t) = 1, \quad A_k(t) = \frac{(\Gamma_3(t))^k}{k!}$$

case c:

$$\Lambda(t) = 1, \quad \Omega(t) = \max_{\tau \in [0, t]} \frac{\mu_3(\tau)}{\mu_2(\tau)}, \quad A_k(t) = \frac{(\Gamma_2(t))^k}{k!}.$$

In case d, one may choose either one of the last two possibilities. Both of them will lead to a correct error bound, though one may be sharper than the other.

In case a, it is easy to check that

$$A'_k(t) = |\mu_1(t)| e^{\Gamma_1(t)} \frac{|\Gamma_1(t)|^{k-1}}{(k-1)!}.$$

Thus, the function  $A_k$  is increasing as a function of  $t$ . This is immediately obvious for cases b-d. This feature of the function  $A_k$  will become important in the proof of the following theorem.

**THEOREM 4.1.** *Suppose that Assumptions 1 and 2 are satisfied for a function  $\sigma(t, s) = \mu_3(t)s$  with  $\mu_3 \in C([0, T], \mathbb{R}_+)$  and suppose that also Assumption 4 is satisfied. Then*

$$(4.3) \quad \|e^k(t)\| \leq (\Lambda(t) + \Omega(t))^k A_k(t) \max_{\tau \in [0, t]} \|e^0(\tau)\|, \quad t \in [0, T], \quad k = 0, 1, 2, \dots$$

*Proof.* Inequality (4.3) is trivially satisfied for  $k = 0$ . We will prove it for  $k > 0$  by induction. First, we consider case a. From (3.10) we have

$$\begin{aligned} \|e^{k+1}(t)\| &\leq e^{\Gamma_1(t)} \int_0^t e^{-\Gamma_1(\tau)} \left[ \frac{\mu_2(\tau)}{|\mu_1(\tau)|} \|e^k(\tau)\| + \frac{\mu_3(\tau)}{|\mu_1(\tau)|} \|e^k_\tau\|_0 \right] |\mu_1(\tau)| d\tau \\ &\leq e^{\Gamma_1(t)} \int_0^t e^{-\Gamma_1(\tau)} [\Lambda(\tau) \|e^k(\tau)\| + \Omega(\tau) \|e^k_\tau\|_0] |\mu_1(\tau)| d\tau. \end{aligned}$$

Now we apply the induction hypothesis to bound the factors  $\|e^k(\tau)\|$  and  $\|e^k_\tau\|_0$ . Since the right-hand side of inequality (4.3) is an increasing function of time, we may write

$$\|e^k_\tau\|_0 \leq (\Lambda(t) + \Omega(t))^k A_k(t) \max_{\tau \in [0, t]} \|e^0(\tau)\|$$

and obtain the following upper bound for  $\|e^{k+1}(t)\|$  :

$$e^{\Gamma_1(t)} \int_0^t e^{-\Gamma_1(\tau)} (\Lambda(\tau) + \Omega(\tau))^{k+1} A_k(\tau) |\mu_1(\tau)| d\tau \max_{\tau \in [0, t]} \|e^0(\tau)\|.$$

This can then be bounded further by

$$(\Lambda(t) + \Omega(t))^{k+1} \text{sign}(\mu_1) e^{\Gamma_1(t)} \int_0^t e^{-\Gamma_1(\tau)} A_k(\tau) \mu_1(\tau) d\tau \max_{\tau \in [0, t]} \|e^0(\tau)\|$$

$$\begin{aligned}
 &= -(\Lambda(t) + \Omega(t))^{k+1} (-\text{sign}(\mu_1))^{k+1} e^{\Gamma_1(t)} \int_0^{\Gamma_1(t)} \left[ e^{-r} - \sum_{j=0}^{k-1} \frac{(-r)^j}{j!} \right] dr \max_{\tau \in [0, t]} \|e^0(\tau)\| \\
 &= (\Lambda(t) + \Omega(t))^{k+1} (-\text{sign}(\mu_1))^{k+1} e^{\Gamma_1(t)} \left[ e^{-\Gamma_1(t)} - \sum_{j=0}^k \frac{(-\Gamma_1(t))^j}{j!} \right] \max_{\tau \in [0, t]} \|e^0(\tau)\|,
 \end{aligned}$$

which proves the theorem.

In the other cases we have  $\Gamma_1 \equiv 0$ . Consider, e.g., case b. From (3.10) we have

$$\|e^{k+1}(t)\| \leq \int_0^t \left[ \frac{\mu_2(\tau)}{\mu_3(\tau)} \|e^k(\tau)\| + \|e_\tau^k\|_0 \right] \mu_3(\tau) d\tau$$

and by the induction hypothesis we obtain

$$\begin{aligned}
 \|e^{k+1}(t)\| &\leq \int_0^t \left( \max_{s \in [0, \tau]} \frac{\mu_2(s)}{\mu_3(s)} + 1 \right)^{k+1} \frac{(\Gamma_3(\tau))^k}{k!} \mu_3(\tau) d\tau \max_{\tau \in [0, t]} \|e^0(\tau)\| \\
 &= \left( \max_{\tau \in [0, t]} \frac{\mu_2(\tau)}{\mu_3(\tau)} + 1 \right)^{k+1} \frac{(\Gamma_3(t))^{k+1}}{(k+1)!} \max_{\tau \in [0, t]} \|e^0(\tau)\|.
 \end{aligned}$$

This, then, proves the theorem. A similar line of reasoning leads to the result for the other cases.  $\square$

**4.2. A special case.** We now consider the case where the qualitative behaviour of the functions  $\mu_1(t)$ ,  $\mu_2(t)$ ,  $\mu_3(t)$  is similar. That is, they are multiples of the same function  $\mu(t)$ , with possibly differing multiplication constants. In the resulting error bounds, the following function depending on three real parameters  $\tilde{\mu}_1$ ,  $\tilde{\mu}_2$ , and  $\tilde{\mu}_3$ , will be useful

$$(4.4) \quad \alpha_k(t) = \begin{cases} \left( \frac{\tilde{\mu}_2 + \tilde{\mu}_3}{-\tilde{\mu}_1} \right)^k \left( 1 - e^{\tilde{\mu}_1 t} \sum_{j=0}^{k-1} \frac{(-\tilde{\mu}_1 t)^j}{j!} \right) & \tilde{\mu}_1 \neq 0 \\ (\tilde{\mu}_2 + \tilde{\mu}_3)^k \frac{t^k}{k!} & \tilde{\mu}_1 = 0 \end{cases}$$

for  $\tilde{\mu}_2, \tilde{\mu}_3 \in \mathbb{R}_+$ . It is easy to check that the expression for  $\tilde{\mu}_1 = 0$  is obtained by taking the limit for  $\tilde{\mu}_1 \rightarrow 0$  of the expression for  $\tilde{\mu}_1 \neq 0$ . Furthermore, when  $\tilde{\mu}_2 + \tilde{\mu}_3 > 0$ , then we have that  $\alpha'_k(0) = 0$  and  $\alpha'_k(t) > 0$  for  $t \in (0, T]$ . Thus,  $\alpha_k$  is increasing as a function of  $t$ .

The following theorem is a special case of Theorem 4.1.

**THEOREM 4.2.** *Suppose that the assumptions of Theorem 4.1 are satisfied with*

$$\mu_i(t) = \tilde{\mu}_i \mu(t), \quad i = 1, 2, 3,$$

where  $\mu \in C([0, T], \mathbb{R}_+)$ ,  $\tilde{\mu}_1 \in \mathbb{R}$  and  $\tilde{\mu}_2, \tilde{\mu}_3 \in \mathbb{R}_+$ . Then

$$(4.5) \quad \|e^k(t)\| \leq \alpha_k(\Gamma(t)) \max_{\tau \in [0, t]} \|e^0(\tau)\|,$$

for  $t \in [0, T]$ ,  $k = 0, 1, 2, \dots$ , where  $\Gamma(t) = \int_0^t \mu(s) ds$ .

*Proof.* In case a, we apply Theorem 4.1 with  $\Lambda(t) = \frac{\tilde{\mu}_2}{|\tilde{\mu}_1|}$ ,  $\Omega(t) = \frac{\tilde{\mu}_3}{|\tilde{\mu}_1|}$ ,  $\Gamma_1(t) = \tilde{\mu}_1 \Gamma(t)$ . In the other cases, we can take either  $\Lambda(t) + \Omega(t) = \frac{\tilde{\mu}_2 + \tilde{\mu}_3}{\tilde{\mu}_3}$ ,  $\Gamma_3(t) = \tilde{\mu}_3 \Gamma(t)$  or  $\Lambda(t) + \Omega(t) = \frac{\tilde{\mu}_2 + \tilde{\mu}_3}{\tilde{\mu}_2}$ ,  $\Gamma_2(t) = \tilde{\mu}_2 \Gamma(t)$ .  $\square$

REMARK 4.1. The inequality in (4.5) originates solely from not keeping the term  $\max_{s \in [0, \tau]} \|e^0(s)\|$  under the integral, but bounding this term by  $\max_{s \in [0, t]} \|e^0(s)\|$ .

REMARK 4.2. In previous analyses of waveform relaxation convergence, one often considers only strict Lipschitz conditions, i.e., constant values for the functions  $\mu_1, \mu_2$ , and  $\mu_3$ . In that case, one has a similar expression as above but with  $\Gamma(t)$  replaced by  $t$ . With time-dependent Lipschitz conditions one has  $\Gamma(t) < t$ . Hence, because  $\alpha_k$  is increasing, we have  $\alpha_k(\Gamma(t)) < \alpha_k(t)$ .

If the function  $\Gamma$  is bounded on  $[0, +\infty)$ , as in Examples 2 and 3, then the function  $\alpha_k(\Gamma(t))$  is also bounded on  $[0, +\infty)$ . The WR error bound in such cases is not only sharper but also independent of time (if the function  $\|e^0(t)\|$  can be bounded by a constant on  $[0, +\infty)$ ). We formulate this observation as a corollary.

COROLLARY 4.1. *Suppose that the assumptions of Theorem 4.2 are satisfied for a function  $\mu$  such that  $\int_0^t \mu(s) ds \leq C_1$ , where  $C_1$  is a constant. Then, for  $t \in [0, \infty)$ ,*

$$(4.6) \quad \|e^k(t)\| \leq \alpha_k(C_1) \max_{\tau \in [0, t]} \|e^0(\tau)\| ,$$

If also  $\|e^0(t)\| \leq C_2$ , with  $C_2$  a constant, then, for  $t \in [0, \infty)$ ,

$$\|e^k(t)\| \leq C_2 \alpha_k(C_1) .$$

Inequality (4.5) leads, by Taylor expansion, to the bound

$$(4.7) \quad \|e^k(t)\| \leq \left( \frac{\tilde{\mu}_2 + \tilde{\mu}_3}{-\tilde{\mu}_1} \right)^k e^{\tilde{\mu}_1 \Gamma(t)} \sum_{j=k}^{\infty} \frac{(-\tilde{\mu}_1 \Gamma(t))^j}{j!} \max_{\tau \in [0, t]} \|e^0(\tau)\| .$$

When  $\mu_1 < 0$ , there is a factor  $e^{\mu_1 \Gamma(t)}$  in (4.7), which is very small for long intervals  $[0, t]$  and large values of  $|\mu_1|$ , see Table 4.1. Such a factor was already mentioned for differential equations without functional argument and under strict Lipschitz conditions in [15]. For delay differential equations the factor  $e^{\mu_1 t}$  also appeared in [1], Theorem 4.3, but only for  $\mu_1 > 0$ . The case  $\mu_1 < 0$  occurs, e.g., when (2.1) arises from the method of lines applied to the partial differential-functional equation (3.4). The magnitude of  $\mu_1$  can be large because of small spatial steps in the difference operators approximating the partial derivatives. For the more general non-constant case considered in Theorem 4.1 this factor is equal to  $e^{\Gamma_1(t)}$ .

Note that the *speed of convergence* does not depend on  $e^{\Gamma_1(t)}$  or  $e^{\mu_1 \Gamma(t)}$ , as there is no dependence on  $k$  in these factors. It depends on the factor  $\Gamma_1(t)$  or  $\Gamma(t)$  which is raised to the power  $k$ .

It is instructive to compare the actual error bounds for certain expressions for the function  $\mu(t)$ . For further reference we mention 4 particular cases considered in the examples in §2:

$$(4.8) \quad \text{if } \mu_i(t) \equiv \tilde{\mu}_i \quad \text{then} \quad \|e^k(t)\| \leq \alpha_k(t) \max_{\tau \in [0, t]} \|e^0(\tau)\| ,$$

$$(4.9) \quad \text{if } \mu_i(t) = \frac{\tilde{\mu}_i}{1 + \lambda t} \quad \text{then} \quad \|e^k(t)\| \leq \alpha_k\left(\frac{1}{\lambda} \ln(1 + \lambda t)\right) \max_{\tau \in [0, t]} \|e^0(\tau)\| ,$$

$$(4.10) \quad \text{if } \mu_i(t) = \frac{\tilde{\mu}_i}{1 + \lambda^2 t^2} \quad \text{then} \quad \|e^k(t)\| \leq \alpha_k\left(\frac{1}{\lambda} \arctan \lambda t\right) \max_{\tau \in [0, t]} \|e^0(\tau)\| ,$$

$$(4.11) \quad \text{if } \mu_i(t) = \tilde{\mu}_i e^{\lambda t} \quad \text{then} \quad \|e^k(t)\| \leq \alpha_k\left(\frac{1}{\lambda} (e^{\lambda t} - 1)\right) \max_{\tau \in [0, t]} \|e^0(\tau)\| .$$

TABLE 4.1

Values of some of the factors appearing in the error bound, corresponding to the  $\mu(t)$ -functions that appear in the examples of §2.2, with  $h = 0.1$ ,  $\mu_1 = -1/4h^2$ , and  $t = 10$ .

$\mu(t)$	Factor $e^{\mu_1 \Gamma(t)}$	Factor $\Gamma(t)$
1	$2.66 \cdot 10^{-109}$	10
$\frac{1}{1+2t}$	$2.96 \cdot 10^{-17}$	1.52
$\frac{1}{1+4t^2}$	$5.54 \cdot 10^{-9}$	0.76
$e^{-\frac{1}{2t}}$	$3.72 \cdot 10^{-6}$	0.5

Some values of certain factors appearing in the error bounds for the examples are calculated and summarized in table 4.1.

**4.3. Illustration and discussion.** We will compare the quality of the estimates obtained with different values for the generalized Lipschitz constants  $\mu_1(t)$ ,  $\mu_2(t)$ , and  $\mu_3(t)$ . We will compare them, in particular, to the actual error obtained in numerical experiments, and to the classical error bounds, i.e., with  $\mu_i(t) = \tilde{\mu}_i$ .

By means of Example 1, we will compare the estimates for  $\mu_i(t) = \tilde{\mu}_i$  to these obtained for  $\mu_i(t) = \frac{\tilde{\mu}_i}{1+\lambda t}$ . In order to illustrate the difference, we first consider the Jacobi/Picard scheme. In that case  $\lambda = 2$  and  $\tilde{\mu}_1 = \frac{-1}{4h^2}$ ,  $\tilde{\mu}_2 = \frac{1}{4h^2}$ ,  $\tilde{\mu}_3 = 1$ , and we take  $h = 0.1$ . The actual error for  $t = 10$ , together with the bounds from (4.8) and (4.9), is shown in the top row of Figure 4.1; we used the Euclidean norm (left) and the infinity norm (right). For these two norms we have

$$\max_{\tau \in [0, t]} \|e^0(\tau)\|_\infty = L^2 t \quad \text{and} \quad \max_{\tau \in [0, t]} \|e^0(\tau)\|_2 \geq 4.358 L^2 t.$$

The same error and bounds, now as a function of  $t$  for a fixed  $k = 20$ , are drawn for the Gauss-Seidel scheme in the second row. In this case  $\tilde{\mu}_1 = \frac{-1}{8h^2}$ ,  $\tilde{\mu}_2 = \frac{1}{8h^2}$ ,  $\tilde{\mu}_3 = 1$ , where  $h = 0.1$ . The third row, shows results for the direct/Picard scheme, namely the error and bounds evaluated at  $t = 10$ .

Next, we consider error estimates for Example 2, which is associated with the bound given in (4.11). In our example  $\lambda = -2$ . For the Gauss-Seidel/Picard scheme the bounds (4.8) and (4.11) are defined with  $\tilde{\mu}_1 = -1/8h^2$ ,  $\tilde{\mu}_2 = 1/8h^2$ , and  $\tilde{\mu}_3 = 2$  for  $h = 0.1$ . The error bounds are compared to the actual error in Figure 4.2. It is worth pointing out that the function  $(e^{\lambda t} - 1)/\lambda$ , which is the argument of  $\alpha_k$ , is bounded by 0.5 on  $[0, +\infty)$ .

For Example 3, we have the bound (4.10) with  $\lambda = 2$ . Note that the argument  $\frac{1}{\lambda} \arctan \lambda t$  is bounded by  $\frac{\pi}{2|\lambda|}$  on the whole of  $[0, +\infty)$ . The bounds for the Gauss-Seidel/Picard scheme, defined with  $\tilde{\mu}_1 = -1/10h^2$ ,  $\tilde{\mu}_2 = 1/10h^2$ , and  $\tilde{\mu}_3 = 1$  for  $h = 0.1$  are drawn together with the actual error in Figure 4.3.

**5. Concluding remarks.** It is possible to derive sharp error bounds for the waveform relaxation technique applied to differential or differential-functional equations with non-constant coefficients. To arrive at these error bounds we considered generalized Lipschitz conditions and derived error estimates by using time-dependent Lipschitz constants. By considering one-sided Lipschitz conditions, we were able to get an error bound that is a factor  $e^{\int_0^t \mu_1(s) ds}$  smaller than the classical error bounds, if the generalized Lipschitz constant  $\mu_1(t)$  is a negative function. This case occurs, e.g., in Jacobi/Picard or Gauss-Seidel/Picard schemes applied to ODEs systems obtained after semidiscretization of parabolic functional equation of the form (3.4). Also, we

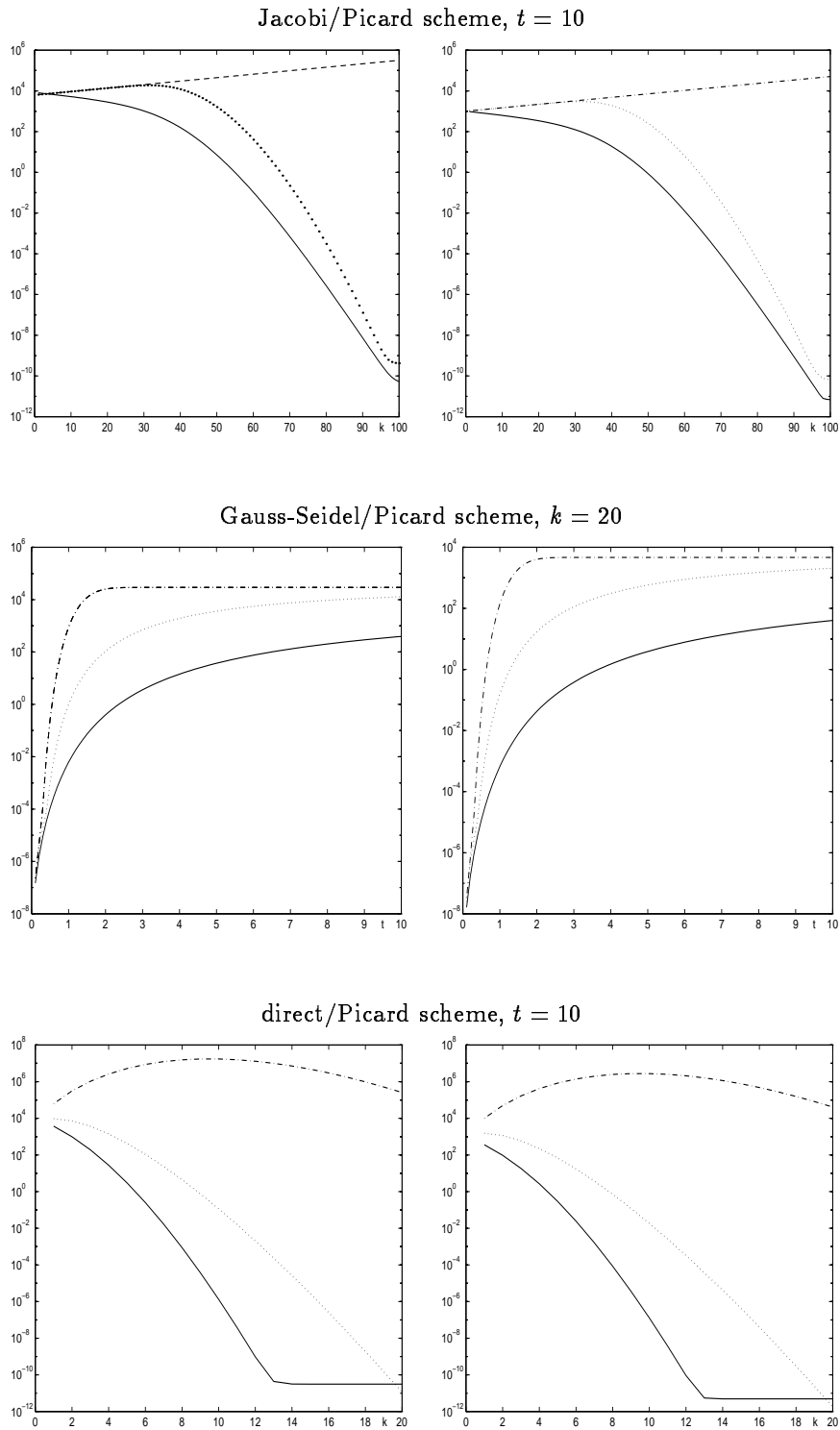


FIG. 4.1. Actual error and error bounds in the Euclidean norm (left) and the infinity norm (right) for the Jacobi/Picard, Gauss-Seidel/Picard and direct/Picard schemes applied to Example 1 ( $L=10$ ,  $M=100$ ,  $h=\Delta t=0.1$ ). Actual error: solid, bound (4.9): dotted, bound (4.8): dashed-dotted.

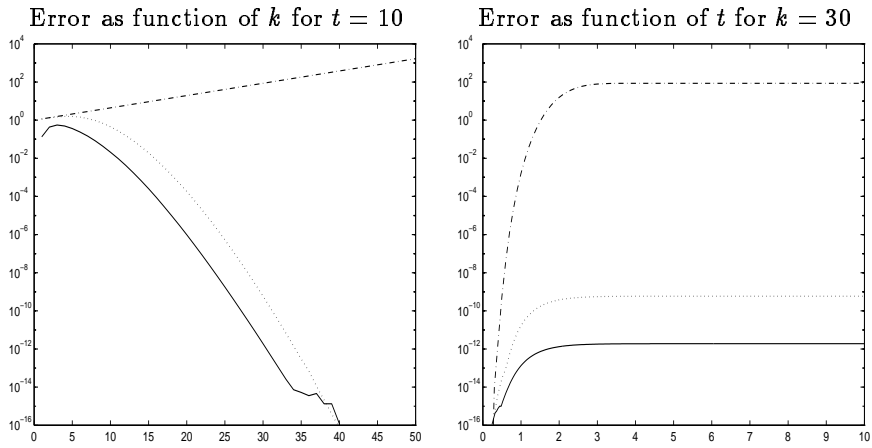


FIG. 4.2. Actual error and error bounds in the infinity norm for the Gauss-Seidel/Picard scheme applied to Example 2. Actual error: solid, bound (4.11): dotted, bound (4.8): dashed-dotted.

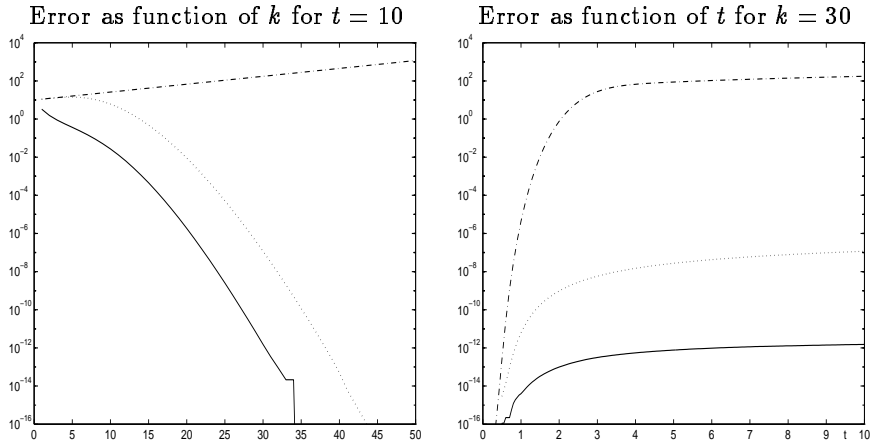


FIG. 4.3. Actual error and error bounds in the infinity norm for the Gauss-Seidel/Picard scheme applied to Example 3. Actual error: solid, bound (4.10): dotted, bound (4.8): dashed-dotted.

were able to produce error bounds that, under certain conditions, are independent of time in the whole interval  $[0, +\infty)$ .

By introducing the generalized Lipschitz constants and the one-sided generalized Lipschitz condition, we were able to derive bounds that are much closer to the actual error, than the ones obtain traditionally. These results were verified by extensive numerical experiments.

Besides offering the potential for good parallel performance, the methods considered in this paper also proved to be very easy to implement. Hence, it is our belief that the waveform relaxation method could become quite an effective numerical method for solving functional differential equations, if the convergence could be improved by using more sophisticated iteration schemes.

REFERENCES

- [1] M. Bjørhus. On dynamic iteration for delay differential equations. *BIT*, 43(3):325–336, 1994.
- [2] M. Bjørhus. A note on the convergence of discretized dynamic iteration. *BIT*, 35(3):291–296, 1995.
- [3] K. Burrage. *Parallel and Sequential Methods for Ordinary Differential Equations*. Oxford University Press, Oxford, 1995.
- [4] A. Feldstein, A. Iserles, and D. Levin. Embedding of delay equations in an infinite-dimensional ODE system. *J. Diff. Eqs*, 117:127–150, 1995.
- [5] J. Hale. *Theory of Functional Differential Equations*. Springer-Verlag, New York, 1977.
- [6] Z. Jackiewicz and M. Kwapisz. Convergence of waveform relaxation methods for differential-algebraic systems. *SIAM J. Numer. Anal.*, 33(6):2303–2317, 1996.
- [7] Z. Jackiewicz, M. Kwapisz, and E. Lo. Waveform relaxation methods for functional differential systems of neutral type. *J. Math. Anal. Appl.*, 207:255–285, 1997.
- [8] V. Lakshmikantham and S. Leela. *Differential and Integral Inequalities*. Academic Press, New York, 1969.
- [9] E. Lelarasme, A. Ruehli, and A. Sangiovanni-Vincentelli. The Waveform Relaxation Method for Time-Domain Analysis of Large Scale Integrated Circuits. *IEEE Trans. CAD*, 1(3):131–145, July 1982.
- [10] E. Lindelöf. Sur l'application des méthodes d'approximations successives à l'étude des intégrales réelles des équations différentielles ordinaires. *J. Math. Pures. Appl.*, 4e série, 10:117–128, 1894.
- [11] U. Mikkala and O. Nevanlinna. Iterative solution of systems of linear differential equations. *Acta Numerica*, pages 259–307, 1996.
- [12] E. Picard. Sur l'application des méthodes d'approximations successives à l'étude de certaines équations différentielles ordinaires. *J. Math. Pures. Appl.*, 4e série, 9:217–271, 1893.
- [13] W. Rudin. *Principles of Mathematical Analysis*. McGraw-Hill, London, 1976.
- [14] J. Sand and K. Burrage. A Jacobi waveform relaxation method for ODEs. *SIAM J. Sci. Computing*, 1998. To appear.
- [15] M. Zennaro. Metodi waveform relaxation per equazioni differenziali ordinarie. *Lecture notes, University of L'Aquila, Italy*, 1992.
- [16] B. Zubik-Kowal. Convergence of the lines method for first - order partial differential - functional equations. *Numer. Meth. Part. Diff. Eqs*, 10:395–409, 1994.
- [17] B. Zubik-Kowal. The method of lines for parabolic differential-functional equations. *IMA J. Num. Anal.*, 17:103–123, 1997.